ANESTHESIOLOGY

Excitation of Putative Glutamatergic Neurons in the Rat Parabrachial Nucleus Region Reduces Delta Power during Dexmedetomidine but not Ketamine Anesthesia

Eric D. Melonakos, Ph.D., Morgan J. Siegmann, B.S., Charles Rey, B.S., Christopher O'Brien, B.S., Ksenia K. Nikolaeva, M.S., Ken Solt, M.D., Christa J. Nehs, Ph.D.

Anesthesiology 2021; 135:633–48

EDITOR'S PERSPECTIVE

What We Already Know about This Topic

- The parabrachial nucleus is an arousal area in the brainstem primarily composed of excitatory glutamatergic neurons
- Stimulation of the parabrachial nucleus reduces cortical delta oscillation power and promotes arousal during or after administration of anesthetics targeting principally the γ-aminobutyric acid type A receptor
- The effects of parabrachial nucleus stimulation on anesthetics with other molecular targets, such as dexmedetomidine or ketamine, are incompletely understood

What This Article Tells Us That Is New

- Chemogenetic excitation of parabrachial excitatory neurons in adult male rats reduced cortical delta power during low-dose dexmedetomidine but not during high-dose dexmedetomidine or ketamine anesthesia
- Changes in cortical delta power did not correspond to changes in time to recovery from anesthesia
- These observations suggest that the effectiveness of parabrachial nucleus excitation to change the neurophysiologic and behavioral effects of anesthesia depends on the molecular mechanisms of actions of general anesthetics

ABSTRACT

Background: Parabrachial nucleus excitation reduces cortical delta oscillation (0.5 to 4 Hz) power and recovery time associated with anesthetics that enhance γ-aminobutyric acid type A receptor action. The effects of parabrachial nucleus excitation on anesthetics with other molecular targets, such as dexmedetomidine and ketamine, remain unknown. The hypothesis was that parabrachial nucleus excitation would cause arousal during dexmedetomidine and ketamine anesthesia.

Methods: Designer Receptors Exclusively Activated by Designer Drugs were used to excite calcium/calmodulin–dependent protein kinase 2α–positive neurons in the parabrachial nucleus region of adult male rats without anesthesia (nine rats), with dexmedetomidine (low dose: 0.3 μg · kg^{-1} · min^{-1} for 45 min, eight rats; high dose: 4.5 μg · kg^{-1} · min^{-1} for 10 min, seven rats), or with ketamine (low dose: 2 mg · kg^{-1} · min^{-1} for 30 min, seven rats; high dose: 4 mg · kg^{-1} · min^{-1} for 15 min, eight rats). For control experiments (same rats and treatments), the Designer Receptors Exclusively Activated by Designer Drugs were not excited. The electroencephalogram and anesthesia recovery times were recorded and analyzed.

Results: Parabrachial nucleus excitation reduced delta power in the prefrontal electroencephalogram with low-dose dexmedetomidine for the 150-min analyzed period, excepting two brief periods (peak median bootstrapped difference [clozapine-*N*-oxide – saline] during dexmedetomidine infusion = –6.06 [99% CI = –12.36 to –1.48] dB, $P = 0.007$). However, parabrachial nucleus excitation was less effective at reducing delta power with high-dose dexmedetomidine and low- and high-dose ketamine (peak median bootstrapped differences during high-dose [dexmedetomidine, ketamine] infusions = [–1.93, –0.87] dB, 99% CI = [–4.16 to –0.56, –1.62 to –0.18] dB, P = [0.006, 0.019]; low-dose ketamine had no statistically significant decreases during the infusion). Recovery time differences with parabrachial nucleus excitation were not statistically significant for dexmedetomidine (median difference for [low, high] dose = [1.63, 11.01] min, 95% CI = [–20.06 to 14.14, –20.84 to 23.67] min, P = [0.945, 0.297]) nor low-dose ketamine (median difference = 12.82 [95% CI: –3.20 to 39.58] min, $P = 0.109$) but were significantly longer for high-dose ketamine (median difference = 11.38 [95% CI: 1.81 to 24.67] min, $P = 0.016$).

Conclusions: These results suggest that the effectiveness of parabrachial nucleus excitation to change the neurophysiologic and behavioral effects of anesthesia depends on the anesthetic's molecular target.

(ANESTHESIOLOGY 2021; 135:633–48)

Despite many advances in recent decades, the mechanisms of general anesthesia–induced unconsciousness remain incompletely understood.[1] One challenge of understanding the mechanisms of anesthesia is that a variety of

This article is accompanied by an editorial on p. 568. Supplemental Digital Content is available for this article. Direct URL citations appear in the printed text and are available in both the HTML and PDF versions of this article. Links to the digital files are provided in the HTML text of this article on the Journal's Web site (www.anesthesiology.org). This article has a visual abstract available in the online version.

Submitted for publication July 11, 2020. Accepted for publication June 14, 2021. Published online first on July 16, 2021. From the Department of Anesthesia, Critical Care and Pain Medicine, Massachusetts General Hospital, Boston, Massachusetts (E.D.M., M.J.S., C.R., C.O., K.K.N., K.S., C.J.N.); the Department of Anaesthesia, Harvard Medical School, Boston, Massachusetts (E.D.M., K.S., C.J.N.); and the Department of Brain and Cognitive Sciences (E.D.M., M.J.S., K.S., C.J.N.) and the Institute for Medical Engineering and Science (K.K.N.), Massachusetts Institute of Technology, Cambridge, Massachusetts.

 Anesthesiology 2021; 135:633–48. DOI: 10.1097/ALN.0000000000003883

<zdoi;. DOI: 10.1097/ALN.0000000000003883>

drugs, with differing molecular and neural circuit targets, each produce the common endpoint of reversible unconsciousness. Among these drugs are propofol, sevoflurane, and isoflurane, each of which potentiate γ-aminobutyric acid receptors; dexmedetomidine, an α_{2A}-adrenergic receptor agonist; and ketamine, which is primarily an *N*-methyl-D-aspartate (NMDA) receptor antagonist.

Despite their differing targets, each of these drugs induces delta oscillations (0.5 to 4 Hz) in the cortical electroencephalogram (EEG). Previous studies have shown that excitation of subcortical arousal areas can be effective at reducing the neural oscillations and behavioral sedation associated with sleep[2–4] or γ-aminobutyric acid–mediated (GABAergic) anesthetics.[5–11] Similarly, delta oscillations and recovery times from GABAergic anesthetics can be reduced by increasing the amounts of arousal area–associated neurotransmitters (or comparable agonists)—acetylcholine (carbachol), norepinephrine, or dopamine—in the brain.[12–16] These findings suggest that these anesthetics may act, at least in part, on endogenous sleep/wake neural circuitry to disrupt consciousness.[17] One such arousal area, the parabrachial nucleus, is primarily composed of glutamatergic neurons and projects to the basal forebrain, amygdala, hypothalamus, thalamus, and cortex.[18,19] Stimulation of the parabrachial nucleus reduces delta oscillation power and promotes arousal during or after administration of propofol, isoflurane, or sevoflurane.[5,8,10] These GABAergic anesthetics are thought to inhibit the parabrachial nucleus and its cortical and subcortical targets, leading to the hypothesis that stimulation of the parabrachial nucleus overcomes the anesthetics' inhibitory effects, promoting neurophysiologic and behavioral arousal.

The effects of parabrachial nucleus stimulation with other anesthetics, such as dexmedetomidine and ketamine, have not yet been described. Some evidence suggests that dexmedetomidine binds to autoreceptors located presynaptically on locus coeruleus neurons, inhibiting norepinephrine release and *dis*inhibiting the preoptic area.[20,21] Because the preoptic area, in turn, inhibits ascending arousal areas, including the parabrachial nucleus, the result is sedation. Other evidence conflicts with this hypothesis,[22–24] and the mechanisms of dexmedetomidine-induced sedation are still being investigated. Ketamine, on the other hand, may inhibit the parabrachial nucleus[25] and its targets, such as the basal forebrain and thalamus,[18,19] *via* its antagonism of NMDA receptors.[26] Simultaneously, ketamine is thought to cause excitation of cortical pyramidal neurons by inhibition of GABAergic interneurons.[27,28] Because the parabrachial nucleus is a target of the preoptic area and a major, glutamatergic arousal nucleus, we hypothesized that parabrachial nucleus stimulation could elicit signs of arousal during both dexmedetomidine- and ketamine-induced unconsciousness. In order to determine the role of this nucleus, we used Designer Receptors Exclusively Activated by Designer Drugs (DREADDs) to selectively stimulate putative glutamatergic neurons in the parabrachial nucleus region of male rats during dexmedetomidine and ketamine anesthesia.

Materials and Methods

Animals

All surgical and experimental protocols were approved by the Massachusetts General Hospital Subcommittee on Research Animal Care, and the Animal Research: Reporting *In Vivo* Experiments (ARRIVE) guidelines were followed. The numbers of subjects for experiments were chosen based on previously published studies of parabrachial nucleus stimulation during anesthesia.[5,8,10] Thirteen adult male Sprague–Dawley rats (Charles River Laboratories, USA) were fed *ad libitum* and housed in rooms with a 12-h light–dark cycle, with lights on at 7 AM and off at 7 PM. All experiments without anesthesia and all anesthesia infusions were completed during the lights-on hours (although some recordings after anesthesia infusions continued past 7 PM). Because previous studies used male rodents to examine the effects of parabrachial nucleus stimulation during anesthesia,[2,5,8,10] we also used male rats.

Surgery

Male rats (~10 weeks old, 312.5 to 409.5 g) were anesthetized using 3% isoflurane followed by maintenance at 2.5% isoflurane (Henry Schein, USA) and placed in a stereotaxic frame (model 942, David Kopf Instruments, USA). The animal's body temperature was maintained at 37°C using a heating pad (50-7220F, Harvard Apparatus, USA). After opening the skin and clearing connective tissue from the top of the skull, craniotomies were made bilaterally over the parabrachial nucleus using a microdrill (Patterson Dental Supply Inc., USA; see fig. 1A for a schematic of craniotomies). A glass micropipette (5-000-1010, Drummond, USA), adapter (MPH6S10, World Precision Instruments, USA), and Hamilton syringe (80301, Hamilton Company, USA) containing the virus (2.8×10^{12} viral genomes/ml, diluted from 2.8×10^{13} viral genomes/ml using saline; pAAV-CaMKIIa-hM3D(Gq)-mCherry; Addgene, USA) for DREADDs transfection were lowered down to the parabrachial nucleus (stereotaxic coordinates, relative to Bregma: −8.0 to −9.06 mm posterior; ±1.96 to ±2.0 mm lateral; −7.2 mm ventral), and 500 nl of virus per side was delivered *via* microinjection pump (53311, Stoelting Co., USA). Three craniotomies were also made over the left prefrontal cortex (2.2 mm posterior; −2.2 mm lateral), left parietal cortex (−3.84 mm posterior; −2.2 mm lateral), and cerebellum (in the middle of the interparietal bone for a reference EEG), and stainless steel EEG electrodes (791400, A-M Systems, USA) were hooked just under the skull at each craniotomy. Finally, holes were drilled for a ground screw over the cerebellum and bone screws (51457, Stoelting Co.) to support the implant. Stainless steel electromyography

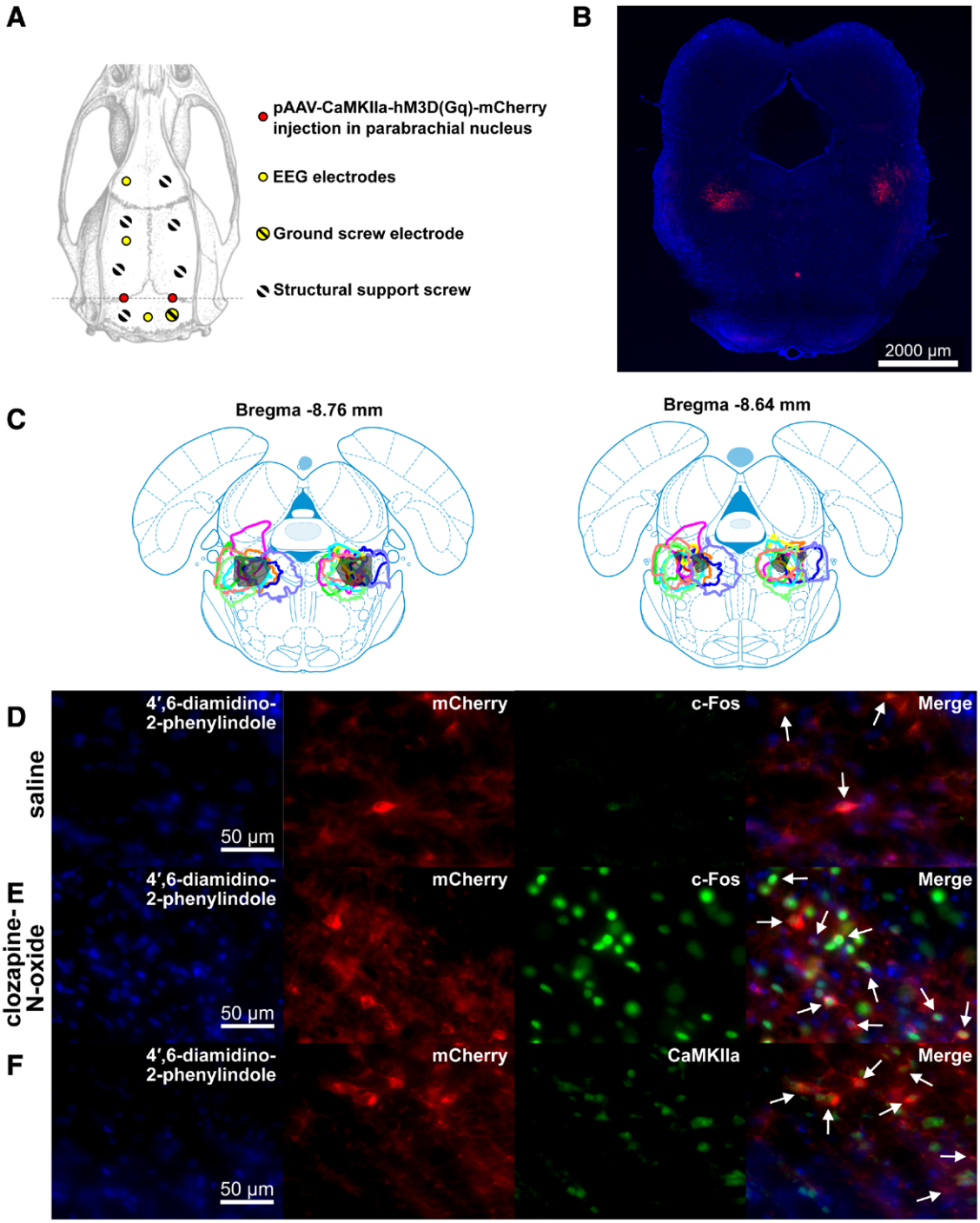

Fig. 1. Overview of electroencephalogram (EEG) electrode locations and Designer Receptors Exclusively Activated by Designer Drugs (DREADDs) expression. (*A*) Schematic of the parabrachial nucleus injection, EEG electrode, and bone screw sites on an overhead view of the rat skull. (*B*) Image showing expression of DREADDs in a coronal slice including the parabrachial nucleus region. (*C*) Outlines of DREADDs expression in the 10 male rats used for the EEG recordings in this study on two different coronal atlas slices including the parabrachial nucleus. Each color indicates a different animal. (*D*, *E*) Immunofluorescence images showing colocalization of c-Fos and DREADDs after saline (*D*) and clozapine-*N*-oxide (*E*) injections. 4′,6-Diamidino-2-phenylindole expression shows cell nuclei in the parabrachial nucleus region. mCherry, a red fluorescent protein, is coexpressed with DREADDs in DREADDs-transfected neurons. Alexa Fluor 488 fluorescence (*green*) shows expression of c-Fos, indicating excited neurons. Merged images show c-Fos expression in mCherry$^+$ (DREADDs$^+$) neurons, indicated by *white arrows*. (*F*) Immunofluorescence image showing colocalization of CaMKIIa and DREADDs. Alexa Fluor 488 fluorescence (*green*) shows expression of CaMKIIa, a marker of glutamatergic neurons. The merged image shows mCherry (DREADDs) expression in CaMKIIa$^+$ neurons, indicated by *white arrows*.

(EMG) electrodes (793500, A-M Systems) were inserted for recording nuchal muscle activity. EEG and EMG electrodes were all connected to a Neuralynx electrode interface board (EIB-8, Neuralynx Inc., USA), and the electrodes and electrode interface board were secured to the skull and bone screws with dental cement. After surgery, the rats were given analgesics (ketoprofen, 4 mg/kg; Ketofen, Zoetis, USA) and allowed to rest for at least 14 days before beginning experiments. This allowed for recovery from surgery and expression of DREADDs. In addition to 10 rats that received the full surgery, three rats were given viral injections only (500 nl or less per side; no EEG/EMG electrode implantation) for histological verification of DREADDs effectiveness and specificity of expression.

Chemogenetics

The excitatory DREADD hM3Dq was used to selectively excite calcium/calmodulin-dependent protein kinase II–positive ($CaMKIIa^+$) neurons. hM3Dq is a muscarinic receptor modified to be sensitive to the exogenous ligand clozapine-*N*-oxide, instead of acetylcholine.[29] We used an adeno-associated virus (AAV8 serotype) that contained a plasmid with a promoter specific to $CaMKIIa^+$ (putative glutamatergic) neurons, followed by the genes for hM3Dq and mCherry, a fluorescent tag (pAAV-CaMKIIa-hM-3D(Gq)-mCherry; Addgene). Using this virus enabled us to constrain expression of hM3Dq to $CaMKIIa^+$ neurons transfected by the virus.

Data Acquisition

EEG (filtered 0.1 to 500 Hz) and EMG (filtered 10 to 500 Hz) signals were acquired using a Neuralynx Digital Lynx SX recording system at a sampling rate of 500 Hz (Neuralynx Inc.). Overhead video recordings were also captured to assess behavioral states.

Study Design

The purpose of this study was to examine the effects of stimulation of the parabrachial nucleus on arousal during dexmedetomidine and ketamine anesthesia. Five anesthesia conditions were paired with saline and clozapine-*N*-oxide injections (for a total of 10 treatment groups): (1) no anesthesia, (2) low-dose dexmedetomidine (0.3 $\mu g \cdot kg^{-1} \cdot min^{-1}$ for 45 min), (3) high-dose dexmedetomidine (4.5 $\mu g \cdot kg^{-1} \cdot min^{-1}$ for 10 min), (4) low-dose ketamine (2 $mg \cdot kg^{-1} \cdot min^{-1}$ for 30 min), and (5) high-dose ketamine (4 $mg \cdot kg^{-1} \cdot min^{-1}$ for 15 min). Each of the subjects of a given anesthesia condition received both clozapine-*N*-oxide and saline injections, in separate experiments, allowing us to compare clozapine-*N*-oxide and saline conditions for each rat. Randomization methods were not used to determine which treatments each rat received or the order in which the treatments (anesthetics or clozapine-*N*-oxide/saline) were received, but the order of experiments was varied between rats (see Supplemental Digital Content 1, http://links.lww.com/ALN/C647, for experiment orders for each rat).

For experiments without anesthesia, intraperitoneal injections of clozapine-*N*-oxide (HY-17366, MedChem Express LLC, USA; and 6329/50, R&D Systems, USA; 1 mg/kg) or saline were given within the half-hour range between 11:23 and 11:53 AM. EEG and EMG were then recorded for 5 h after the injection. For these experiments without anesthesia, the rats were allowed to rest for at least 3 days between experiments if clozapine-*N*-oxide was given in the first of the two experiments and at least 1 day if saline was given first.

For experiments with anesthesia, before starting recordings, the rats were anesthetized with isoflurane for ~15 min to place an intravenous port in the lateral tail vein. Immediately after cessation of isoflurane, clozapine-*N*-oxide (or saline) intraperitoneal injections were administered. One hour after the clozapine-*N*-oxide (or saline) injection, dilutions of dexmedetomidine (2 μg/ml for low dose or 5 μg/ml for high dose; dexmedetomidine hydrochloride injection, Sun Pharmaceutical Industries, India; and dexmedetomidine injection, Accord Healthcare, India) or ketamine (6 mg/ml; ketamine HCl injection, West-Ward, USA) in saline were administered intravenously *via* a syringe pump (HA3000I, Harvard Apparatus). This time delay allowed for clozapine-*N*-oxide to reach its maximal effectiveness, which occurs at ~45 min after administration.[30] Two exceptions to the 1-h delay between clozapine-*N*-oxide (or saline) and anesthetic infusion occurred: in one high-dose dexmedetomidine experiment (rat 4), clozapine-*N*-oxide was injected 140 min before the start of the anesthetic infusion, and in one high-dose ketamine experiment (rat 3), saline was injected 116 min before the start of the anesthetic infusion. Both exceptions were well within the ~9-h period during which clozapine-*N*-oxide has been shown to be effective.[30] Normothermia was maintained with a heating pad under the recording cage while the animals were anesthetized. EEG and EMG recordings were started a minimum of 10 min before beginning anesthesia infusion. The rats were allowed to rest for at least 3 days between all experiments with anesthesia except one high-dose ketamine experiment. Only 2 days of rest were given before that experiment, because it followed an aborted ketamine experiment in which the IV started leaking before the infusion completed. For experiments with anesthesia, recordings continued until the rats recovered from anesthesia and were mobile.

After completion of each subject's experiments, the rats were euthanized using isoflurane overdose and exsanguination *via* transcardial perfusion (see "Histology"). Blinding methods were not used in this study.

Analysis of Sleep States

The EEG and EMG signals from experiments without anesthesia were used to visually score wakefulness, non–rapid-eye-movement (non-REM) sleep, and rapid-

eye-movement (REM) sleep in 2-s epochs using Spike2 (CED, United Kingdom). The time spent in waking, non-REM, and REM sleep were then separately totaled over the 5 h after saline or clozapine-*N*-oxide injection. Each rat's state was assumed to be awake during the first few minutes after their injection, because it took a few minutes of active handling to plug them into the recording system.

Analysis of Recovery Times

Just after the anesthetic infusion finished, each rat was turned on its side. Recovery time was measured as the time from the end of the anesthetic infusion to when the rat righted itself and had all four paws on the floor. In five of the low-dose dexmedetomidine experiments, the rats never lost the righting reflex; in such cases, return of movement was used to measure recovery time.

Spectral Analysis of EEG Data

The data were analyzed using MATLAB (Mathworks, USA). Before spectral analysis, the mean of each EEG recording was subtracted from the entire signal. Artifacts were then removed by identifying time points where the voltage crossed a threshold of ±1,500 μV. All threshold crossings less than 1 min apart were grouped together as a single artifact, with all time points in between treated as threshold crossings. The signal at and surrounding each of these time points was then multiplied by an inverted Hamming window with a length of 0.15 s, centered at the identified voltage threshold crossing. In this manner, time points identified as threshold crossings were set to 0 μV, and the signal 0.075 s before and after artifacts gradually increased to full magnitude, reducing sharp edges in the signal that would produce harmonics in the spectrogram.

All spectrograms in this study were computed using the multitaper methods described by Prerau *et al.*[31] Example spectrograms were computed from 0 to 30 Hz (for experiments without anesthesia) or 0 to 50 Hz (for experiments with anesthesia) using a 30-s window that moved in 3-s steps, a time-half-bandwidth product of 3, and five discrete prolate spheroidal sequence tapers. The signal in each window was linearly detrended before the multitaper spectrogram was computed. For Supplemental Digital Content 2–6 (http://links.lww.com/ALN/C649, http://links.lww.com/ALN/C650, http://links.lww.com/ALN/C651, http://links.lww.com/ALN/C652, http://links.lww.com/ALN/C653), the spectrograms were computed from 0 to 60 Hz (to accommodate gamma band analysis) for both experiments with and without anesthesia. Any windows with 0 μV^2 total power, such as those comprised solely of removed electrical artifacts, were discarded from the analysis (*e.g.*, see the beginning of the spectrograms in fig. 2 [A and B], in which the artifact time points are given the color of the minimum value in the spectrogram), and power was converted to dB.

Statistical Analysis

All statistical analyses were performed using MATLAB, unless otherwise noted. To measure the power in various frequency bands between conditions over time, the multitaper spectrogram was computed from 0 to 30 Hz (for experiments without anesthesia) or 0 to 50 Hz (for experiments with anesthesia) using a 120-s, nonoverlapping time window, a time-half-bandwidth product of 3, and five discrete prolate spheroidal sequence tapers. The signal in each window was linearly detrended before the multitaper spectrogram was computed. After discarding windows with 0 μV^2 total power and conversion to dB, the power in each band (delta: 0.5 to 4 Hz; theta: 4 to 8 Hz; alpha: 10 to 15 Hz; beta: 15 to 30 Hz; and gamma: 40 to 60 Hz) was averaged for each time point in the spectrogram. This mean power was aligned in time for all rats, relative to the start of anesthesia delivery.

For comparison of mean power in each frequency band between clozapine-*N*-oxide and saline conditions, because of the small sample sizes, we used the bootstrapping technique to find the CI values. For each time point, the mean spectral power in a given frequency band from the saline condition was subtracted from the corresponding time point's power in the clozapine-*N*-oxide condition of the same rat. The differences from all rats for each time point were sampled with replacement N times (where N = the number of subjects), and the mean was taken. This process was repeated 5,000 times for each time point to form a bootstrapped collection of 5,000 mean power differences. From this bootstrapped collection, the overall median for each time point was taken, and 99% CIs were found by taking the range containing 99% of the bootstrapped mean differences. Thus, when then the CIs do not overlap with 0, it indicates 99% confidence that there is a difference between the mean power in that frequency band under clozapine-*N*-oxide and saline conditions. *P* values that are reported for times with peak median bootstrapped mean differences in power were calculated by rerunning the bootstrap analysis for those time points using the "boot.t.test" function in the MKinfer package (version 0.6) in *R* (version 4.1.0; 99% confidence level, 5,000 bootstrap replicates; reported medians and CIs for peak median bootstrapped differences in power were taken from the MATLAB bootstrap analysis described above). For some figure panels containing bootstrapped mean differences in power (figs. 2C, 3B, 5B, and 6B, and the associated Supplemental Digital Content 2–6 [http://links.lww.com/ALN/C649, http://links.lww.com/ALN/C650, http://links.lww.com/ALN/C651, http://links.lww.com/ALN/C652, http://links.lww.com/ALN/C653]), the number of subjects (N) at each time point varies because of occasional electrical artifacts, so ranges of N are reported. For figure 2C, the first 10 min of measurements after clozapine-*N*-oxide or saline injections (at time = 0) were not used to calculate the reported range of N, because some rats took longer than others to plug into the EEG recording system.

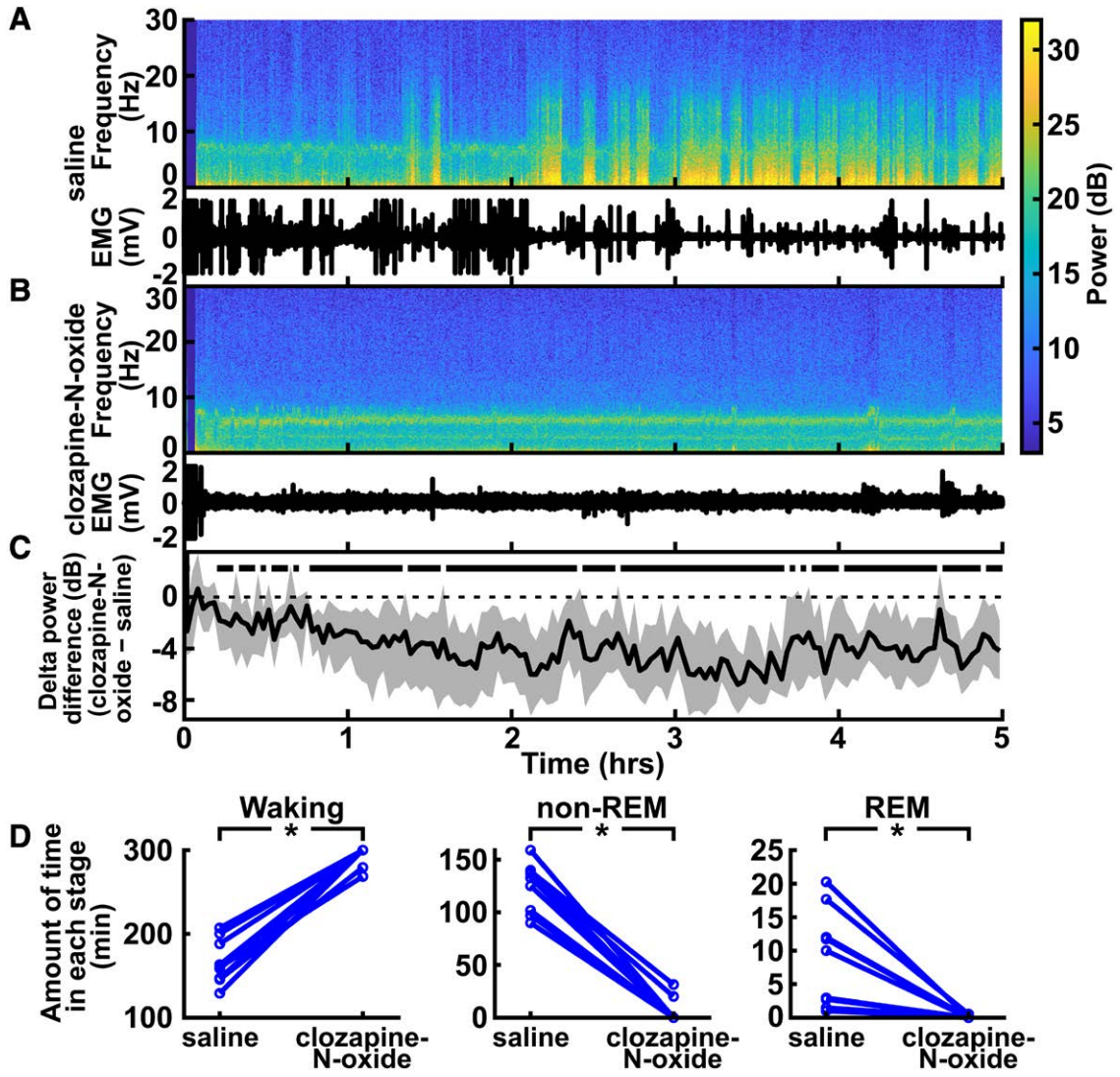

Fig. 2. Excitation of CaMKIIa+ neurons in the parabrachial nucleus region decreased delta oscillations, non–rapid-eye-movement (non-REM), and REM sleep without anesthesia. (*A*) An example spectrogram shows the spectral power for 0 to 30 Hz over time in the prefrontal electroencephalogram after intraperitoneal injection of saline (*top*). The electromyography (EMG) from the same experiment shows a lack of movement during times with high delta power (*bottom*). (*B*) An example spectrogram from the same rat after clozapine-*N*-oxide injection shows an absence of high delta power (*top*). The corresponding EMG shows stillness, possibly due to the clozapine-*N*-oxide injection (*bottom*; see "Discussion"). (*C*) Summary of power differences between conditions over time shows decreased mean delta power for clozapine-*N*-oxide experiments relative to saline experiments. For all power difference traces in this and subsequent figures, the traces represent the median (±99% CI) of a bootstrapped collection of 5,000 mean differences. Thus, time points where the CIs (*shaded regions*) do not overlap with zero show statistically significant differences with 99% confidence. Time periods that show statistically significant differences with 99% confidence are indicated by *black bars* above the *dashed zero line*, representing lower power in the clozapine-*N*-oxide condition. Saline or clozapine-*N*-oxide injections were given at time 0 h. (*A*) through (*C*) have the same time axes. (*D*) Comparison of the amount of time spent in waking (*left*), non-REM (*middle*), and REM (*right*) stages between saline and clozapine-*N*-oxide conditions for the 5 h after injection. Time spent in waking was longer and time spent in non-REM and REM sleep was shorter with clozapine-*N*-oxide experiments, relative to saline experiments, in a statistically significant way. **P* < 0.05, two-sided Wilcoxon signed-rank test.

For statistical comparison of the time spent in each sleep stage (for experiments without anesthesia) or the recovery times (for experiments with anesthesia), we used *R* (version 4.1.0). The reported median differences for these measurements are Hodges–Lehmann estimates. Because the same animals received both clozapine-*N*-oxide and saline conditions, we used the two-sided Wilcoxon signed-rank test with an α value of 0.05 to determine statistical significance. The Wilcoxon signed-rank tests, the median differences, and the 95% CIs were calculated using the "wilcox.test" function in *R*.

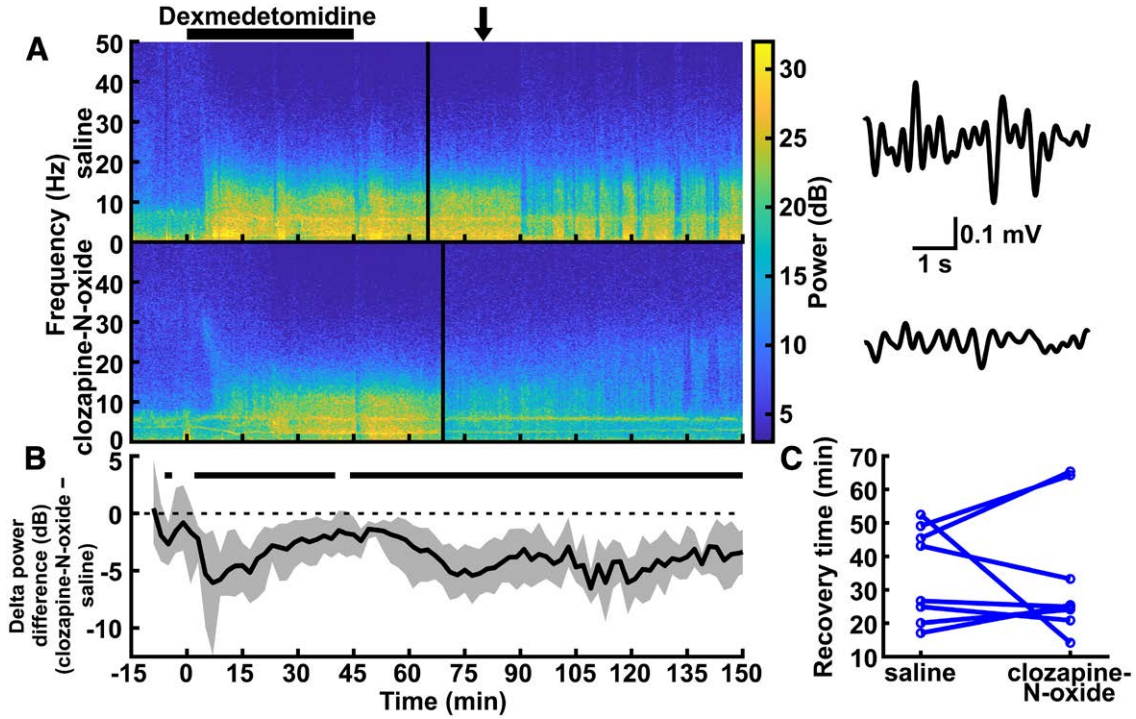

Fig. 3. Excitation of CaMKIIa+ neurons in the parabrachial nucleus region decreased delta oscillations but did not affect recovery time with low-dose dexmedetomidine anesthesia. (*A*) Example spectrograms showing the spectral power for 0 to 50 Hz over time in the prefrontal electroencephalogram after intraperitoneal injections of saline (*top*) and clozapine-*N*-oxide (*bottom*) in the same rat. *Black bars* over the spectrograms indicate the time when the dexmedetomidine infusion (0.3 μg · kg^{-1} · min^{-1} for 45 min) took place. Clozapine-*N*-oxide or saline injections were given an hour before the start of dexmedetomidine infusion. *Solid vertical lines* represent the time of recovery for each example experiment. (Note: the transient dip in delta power at the end of dexmedetomidine administration in both [*A*] and [*B*] is due to our handling the rat to place it on its side.) Example electroencephalogram traces to the *right* of each spectrogram are bandpass-filtered from 0.5 to 4 Hz and show the reduced delta amplitude with parabrachial nucleus region excitation. The *arrow* over the spectrograms indicates the time, for both conditions, when the traces were taken. (*B*) Summary of power differences over time shows decreased mean delta power for clozapine-*N*-oxide experiments relative to saline experiments. Time periods that show statistically significant differences with 99% confidence are indicated by *black bars* above the *dashed zero line*, representing lower power in the clozapine-*N*-oxide conditions. The spectrograms in (*A*) and summary power in (*B*) have the same time axes. (*C*) No statistically significant differences between conditions were seen in recovery times, as measured by time to return of righting reflex (or return of movement in cases where righting reflex was not lost).

Histology

After completion of experiments, the rats were euthanized with isoflurane (5%) and transcardially perfused with 1[times] phosphate-buffered saline, followed by 10% formalin. The brains were then sliced at 50 μm using a vibratome (VT1000 S, Leica Biosystems, USA). The slices were mounted on a slide with a 4′,6-diamidino-2-phenylindole–containing mounting medium (H-1200-10, Vector Laboratories, USA). The brain slices were imaged using a fluorescence microscope (Axio Imager.M2, Zeiss, USA) to localize expression of mCherry/DREADDs in the parabrachial nucleus region (fig. 1, B and C).

In addition, immunofluorescence was used in a subset of animals to confirm the effectiveness of DREADDs stimulation and the specificity of DREADDs expression to CaMKIIa+ neurons (fig. 1, D through F, respectively). To confirm DREADDs effectiveness, we injected rats with clozapine-*N*-oxide or saline 60 to 70 min before euthanasia. Perfusion and slicing occurred as mentioned above, followed by immunofluorescence. For the immunofluorescence, the brain slices were first rinsed in phosphate-buffered saline for 5 to 10 min three times. A solution consisting of 0.1% Triton X-100 (Boston BioProducts, USA) in phosphate-buffered saline was used as the bulk solution for a blocking solution containing 10% normal goat serum (ab7481, Abcam, United Kingdom) and 4% bovine serum albumin (001-000-161, Jackson ImmunoResearch, USA). The slices were placed in this blocking solution for 1 h. The slices were then incubated overnight at room temperature in blocking solution with an anti–c-Fos primary antibody (1:2,000; 226003, Synaptic Systems, Germany).

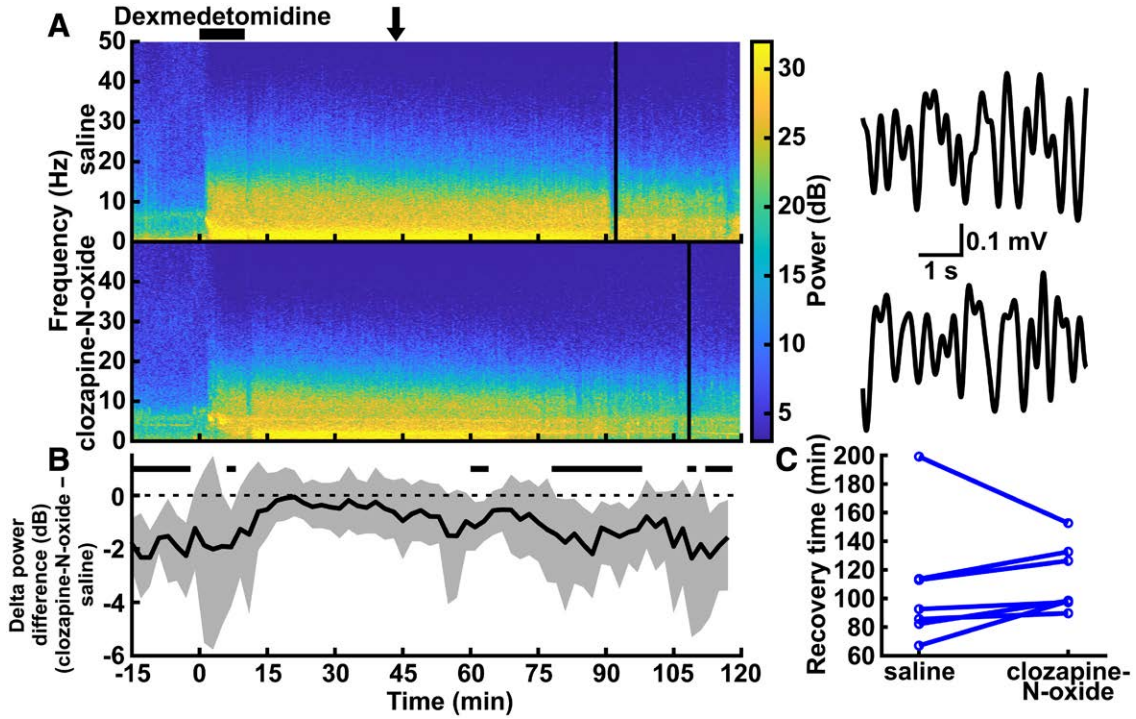

Fig. 4. Excitation of CaMKIIa$^+$ neurons in the parabrachial nucleus region only caused minor reductions in delta oscillations and did not affect recovery time with high-dose dexmedetomidine anesthesia. (*A*) Example spectrograms showing the spectral power for 0 to 50 Hz over time in the prefrontal electroencephalogram after intraperitoneal injections of saline (*top*) and clozapine-*N*-oxide (*bottom*) in the same rat. The *black bar* over the spectrograms indicates the time when the dexmedetomidine infusion (4.5 μg · kg^{-1} · min^{-1} for 10 min) took place. Clozapine-*N*-oxide or saline injections were given before the start of the dexmedetomidine infusion. A *solid vertical line* represents the time of recovery for each example experiment. (Note: the transient dip in delta power at the end of dexmedetomidine administration in both [*A*] and [*B*] is due to our handling the rat to place it on its side.) Example electroencephalogram traces to the *right* of each spectrogram are bandpass-filtered from 0.5 to 4 Hz and show similar delta amplitude with and without parabrachial nucleus region excitation. The *arrow* over the spectrograms indicates the time, for both conditions, when the traces were taken. (*B*) Summary of power differences over time shows minor decreases in delta power for clozapine-*N*-oxide experiments relative to saline experiments. Time periods that show statistically significant differences with 99% confidence are indicated by *black bars* above the *dashed zero line*, representing lower power in the clozapine-*N*-oxide condition. Spectrograms in (*A*) and summary power in (*B*) have the same time axes. (*C*) No statistically significant differences between conditions were seen in recovery times, as measured by time to return of righting reflex.

After incubation, the slices were rinsed in phosphate-buffered saline or 0.1% Triton X-100 for 5 to 10 min three times and then allowed to incubate for 2 h at room temperature in blocking solution with Alexa Fluor 488 secondary antibodies (1:200; A-11008, Invitrogen, USA). Finally, the slices were rinsed twice in 0.1% Triton X-100 and then twice more with phosphate-buffered saline (without Triton X-100) and mounted on a slide with a 4′,6-diamidino-2-phenylindole–containing mounting medium.

To confirm the specificity of DREADDs expression to CaMKIIa$^+$ neurons, the brain slices were first rinsed in 0.3% Triton X-100 in phosphate-buffered saline for 5 to 10 min three times. This solution was used as the bulk solution for a blocking solution containing 10% normal donkey serum (S30-100ML, EMD Millipore, USA). The slices were placed in the blocking solution for 1 h. Then the slices were incubated overnight at 4°C in blocking solution with an anti-CaMKIIa primary antibody (1:50; PA5-19128, Invitrogen). After incubation, the slices were rinsed in 0.3% Triton X-100 for 5 to 20 min three times and then allowed to incubate for 2 h at room temperature in blocking solution with Alexa Fluor 488 secondary antibodies (1:200; 705-545-003, Jackson ImmunoResearch). Finally, the slices were rinsed twice in 0.3% Triton X-100 and then twice more with phosphate-buffered saline (without Triton X-100) and mounted on a slide with a 4′,6-diamidino-2-phenylindole–containing mounting medium.

All washes and incubations for both immunofluorescence protocols were performed with free-floating brain slices in 12- or 24-well plates placed on a rocker. Colocalization of mCherry, indicating DREADDs expression, and Alexa Fluor 488, indicating c-Fos or CaMKIIa expression, was

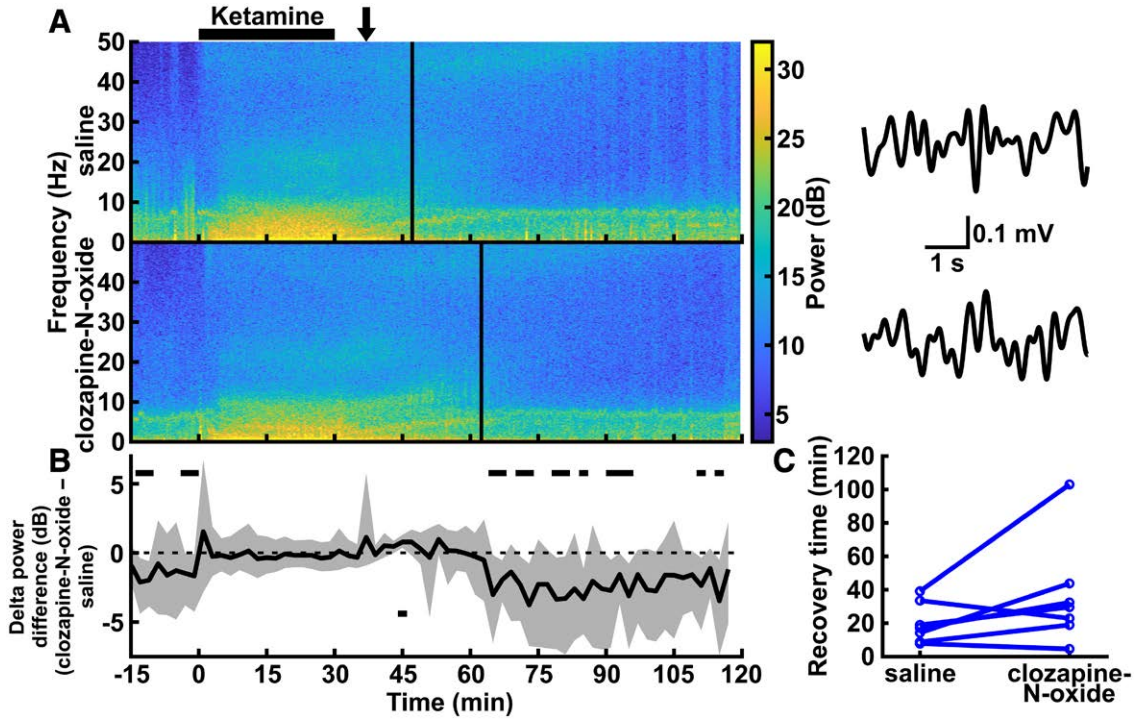

Fig. 5. Excitation of CaMKIIa+ neurons in the parabrachial nucleus region did not affect delta oscillations during, nor the recovery time after, low-dose ketamine anesthesia. (*A*) Example spectrograms showing the spectral power for 0 to 50 Hz over time in the prefrontal electroencephalogram after intraperitoneal injections of saline (*top*) and clozapine-*N*-oxide (*bottom*) in the same rat. A *black bar* over the spectrograms indicates the time when the low-dose ketamine infusion (2 mg · kg^{-1} · min^{-1} for 30 min) took place. Clozapine-*N*-oxide or saline injections were given an hour before the start of the ketamine infusion. A *solid vertical line* represents the time of recovery for each example experiment. Example electroencephalogram traces to the *right* of each spectrogram are bandpass-filtered from 0.5 to 4 Hz and show similar delta amplitude with and without parabrachial nucleus region excitation. The *arrow* over the spectrograms indicates the time, for both conditions, when the traces were taken. (*B*) Summary of power differences over time shows similar delta power for clozapine-*N*-oxide and saline experiments during ketamine infusions. Time periods that show statistically significant differences with 99% confidence are indicated by *black bars* above or below the *dashed zero line*, representing lower power in the clozapine-*N*-oxide or saline conditions, respectively. The spectrograms in (*A*) and summary power in (*B*) have the same time axes. (*C*) No statistically significant differences between conditions were seen in recovery times, as measured by time to return of righting reflex.

then visualized using the Zeiss microscope mentioned previously. Neurons with and without colocalized fluorescence were counted using Fiji software.[32]

Results

We tested the effects of exciting putative glutamatergic neurons in the parabrachial nucleus by using DREADDs (hM3Dq) and surgically implanted EEG electrodes (fig. 1A). Excitatory DREADDs were expressed in the parabrachial nucleus and in the surrounding region, especially rostral to the parabrachial nucleus (see example expression in fig. 1B and a summary of expression across all 10 rats in two atlas slices in fig. 1C; a summary of mCherry expression across a range of atlas slices is shown in Supplemental Digital Content 7, http://links.lww.com/ALN/C648). Effectiveness of DREADDs stimulation was confirmed by intraperitoneally injecting clozapine-*N*-oxide, the ligand for DREADDs, and then using immunofluorescence to confirm expression of c-Fos, a marker of neural activity (fig. 1, D and E; 4 of 54 DREADDs+ neurons were c-Fos+ after a saline control injection, N = 1 male rat; 100 of 124 counted DREADDs+ neurons were c-Fos+ after clozapine-*N*-oxide injections, N = 2 male rats). The specificity and extent of DREADDs expression in CaMKIIa+ neurons were also confirmed using immunofluorescence (fig. 1F; inside the parabrachial nucleus: 333 of 383 counted DREADDs+ neurons were CaMKIIa+, and in the same fields of view, 333 of 778 counted CaMKIIa+ neurons were DREADDs+, N = 3 male rats; outside the parabrachial nucleus: 128 of 173 counted DREADDs+ neurons were CaMKIIa+, and in the same fields of view, 128 of 956 counted CaMKIIa+ neurons were DREADDs+, N = 1 male rat). Thus, by intraperitoneally injecting clozapine-*N*-oxide, the ligand for

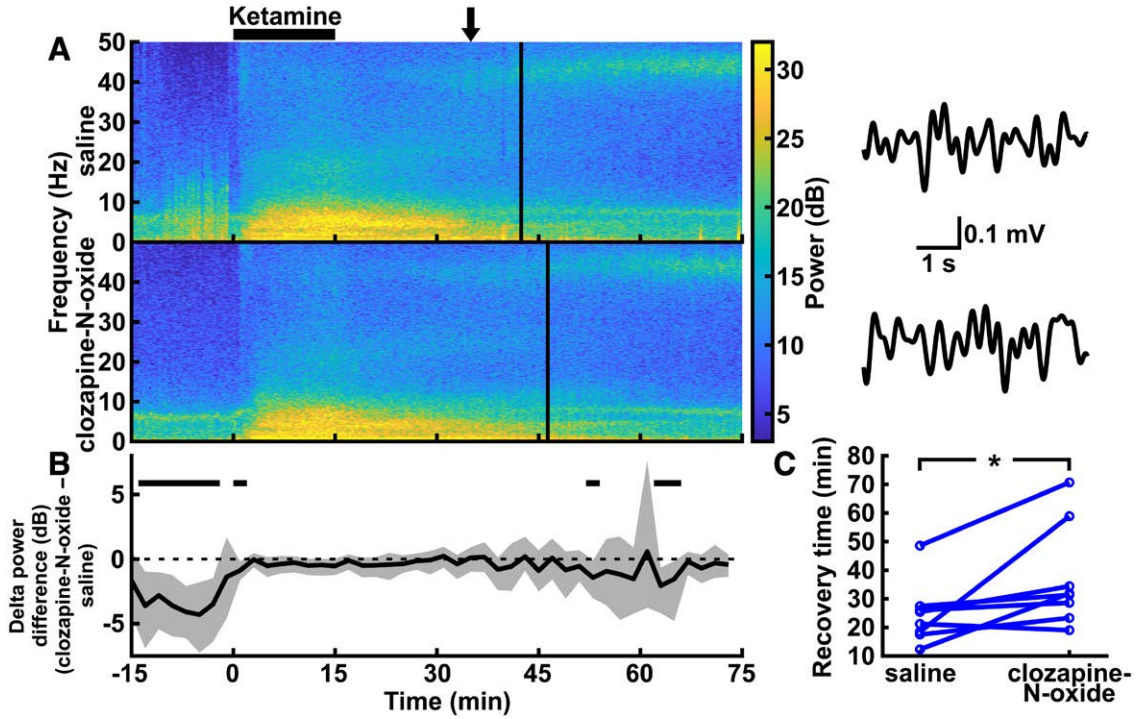

Fig. 6. Excitation of CaMKIIa$^+$ neurons in the parabrachial nucleus region had minor effects on delta oscillations and prolonged recovery time with high-dose ketamine anesthesia. (*A*) Example spectrograms showing the spectral power for 0 to 50 Hz over time in the prefrontal electroencephalogram after intraperitoneal injections of saline (*top*) and clozapine-*N*-oxide (*bottom*) in the same rat. *Black bars* over the spectrograms indicate the times when the high-dose ketamine infusion (4 mg · kg^{-1} · min^{-1} for 15 min) took place. Clozapine-*N*-oxide or saline injections were given before the start of the ketamine infusion. A *solid vertical line* represents the time of recovery for each example experiment. Example electroencephalogram traces to the *right* of each spectrogram are bandpass-filtered from 0.5 to 4 Hz and show similar delta amplitudes with and without parabrachial nucleus region excitation. The *arrow* over the spectrograms indicates the time, for both conditions, when the traces were taken. (*B*) Summary of power differences over time shows similar delta power, other than a few transient decreases, for clozapine-*N*-oxide experiments relative to saline experiments. Time periods that show statistically significant differences with 99% confidence are indicated by *black bars* above the *dashed zero line*, representing lower power in the clozapine-*N*-oxide condition. The spectrograms in (*A*) and summary power in (*B*) have the same time axes. (*C*) Recovery time from high-dose ketamine anesthesia, as measured by time to return of righting reflex, was longer with clozapine-*N*-oxide experiments, relative to saline experiments, in a statistically significant way. *$P < 0.05$, two-sided Wilcoxon signed-rank test.

DREADDs, we were able to selectively excite CaMKIIa$^+$ neurons during conditions without anesthesia or with dexmedetomidine or ketamine anesthesia.

Some experimental data were not included in our analyses, despite being collected (see grayed-out experiments in Supplemental Digital Content 1, http://links.lww.com/ALN/C647). These included a low-dose ketamine experiment in which the clozapine-*N*-oxide never fully dissolved (rat 1) and a high-dose dexmedetomidine experiment in which the rat (rat 3) was clearly aroused by a neighboring rat's tail flick. In addition, two rats experienced issues that prevented them from completing all the planned experiments: rat 2's electrode interface board broke during an experiment without anesthesia, and rat 5 suffered from painful limb swelling that confounded the measurement of recovery time during a low-dose dexmedetomidine experiment. These issues led to the euthanasia of these two rats and thus prevented them from completing the low-dose anesthesia experiments. Two other rats, rats 8 and 10, were not included in the high-dose dexmedetomidine and high-dose ketamine treatment groups after we felt we had sufficient data to characterize the effects of parabrachial nucleus stimulation during those anesthetics and doses. Finally, after histological analysis, it was found that one rat that was initially included in experiments did not express DREADDs in the parabrachial nucleus and was thus not included in any of our analyses. One other rat did not survive the initial surgery and was not used for any experimental treatment groups.

Excitation of CaMKIIa$^+$ Neurons in the Parabrachial Nucleus Region Reduces Delta Power without Anesthesia

Previous research has shown that nonspecific excitation of parabrachial nucleus neurons decreases the delta power

associated with the awake and non-REM sleep states (indicating neurophysiologic arousal), without anesthesia.[2] Because the parabrachial nucleus is primarily glutamatergic, we first tested whether specific excitation of CaMKIIa$^+$ neurons also promotes arousal under these conditions. We measured delta power (0.5 to 4 Hz) in the prefrontal EEG for the first 5 h after an intraperitoneal injection of clozapine-*N*-oxide (1 mg/kg). In congruence with the effects of nonspecific parabrachial nucleus excitation, we observed reduced delta power relative to control conditions in which intraperitoneal injections of saline were administered to the same rats (fig. 2; trace in fig. 2C summarizes delta power with clozapine-*N*-oxide injections minus delta power with saline injections, and periods with CIs that do not span zero show statistically significant differences with 99% confidence; peak statistically significant median bootstrapped difference in power [clozapine-*N*-oxide – saline] = –6.79 dB, 99% CI = –9.05 to –4.16 dB, P = 0.001, N = 9 male rats; for entire trace in fig. 2C, N = 8 to 9 male rats). Whereas the EEG under saline control conditions showed increased delta power, reflecting an increase in sleeping over time, the delta power with clozapine-*N*-oxide injections remained at awake levels. Power in other frequency bands, including theta (4 to 8 Hz), alpha (10 to 15 Hz), and beta (15 to 30 Hz), likewise decreased with clozapine-*N*-oxide injections relative to saline injections. Conversely, power in the gamma band (40 to 60 Hz) increased with clozapine-*N*-oxide injections (see Supplemental Digital Content 2, http://links.lww.com/ALN/C649, which shows the summary power differences [clozapine-*N*-oxide – saline] for the theta, alpha, beta, and gamma bands).

Moreover, a formal assessment of sleep states during the 5 h after clozapine-*N*-oxide injections shows decreased time spent in non-REM and REM sleep relative to experiments with saline injections (fig 2D; median difference in time spent waking [clozapine-*N*-oxide – saline] = 126.31 min, 95% CI = 104.13 to 152.31 min, P = 0.004; median difference in time spent in non-REM sleep [clozapine-*N*-oxide – saline] = –117.23 min, 95% CI = –137.74 to –99.39 min, P = 0.004; median difference in time spent in REM sleep [clozapine-*N*-oxide – saline] = –9.07 min, 95% CI = –15.13 to –2.10 min, P = 0.004; N = 9 male rats). These results suggest that excitation of CaMKIIa$^+$ neurons alone in the parabrachial nucleus region is sufficient to reduce delta power and sleep in male rats without anesthesia, consistent with increased arousal.

Excitation of CaMKIIa$^+$ Neurons in the Parabrachial Nucleus Region Reduces Delta Power during Low-dose, but Not High-dose, Dexmedetomidine Anesthesia

Excitation of the parabrachial nucleus, including selective excitation of glutamatergic neurons,[8] is effective at reducing both delta oscillations and the time to recovery from isoflurane, sevoflurane, and propofol anesthesia.[5,10] We tested whether excitation of CaMKIIa$^+$ neurons in the parabrachial nucleus region has similar effects with dexmedetomidine or ketamine. One hour after injection of clozapine-*N*-oxide, we administered dexmedetomidine (0.3 $\mu g \cdot kg^{-1} \cdot min^{-1}$ for 45 min). We found that delta power in the prefrontal EEG was reduced relative to control experiments in the same rats with saline injections. This reduction was statistically significant between 2 and 40 min after the start of the infusion and from 44 min until the end of the analyzed period (150 min; fig. 3, A and B; trace in fig. 3B summarizes delta power with clozapine-*N*-oxide injections minus delta power with saline injections, and periods with CIs that do not span zero show statistically significant differences with 99% confidence; peak statistically significant median bootstrapped difference in power during dexmedetomidine infusion [clozapine-*N*-oxide – saline] = –6.06 dB, 99% CI = –12.36 to –1.48 dB, P = 0.007, N = 8 male rats; for the entire trace in fig. 3B, N = 7 to 8 male rats). Consistent with experiments without anesthesia (fig. 2), there was also some statistically significant reduction in delta power before the start of anesthesia. Power in the theta, alpha, and beta frequency bands likewise decreased with clozapine-*N*-oxide injections relative to saline injections. The prevalence of these decreases across the recorded period declined as the frequency of the band increased (*i.e.*, theta > alpha > beta). Conversely, power in the gamma band had slight increases with clozapine-*N*-oxide injections (see Supplemental Digital Content 3, http://links.lww.com/ALN/C650, which shows the summary power differences [clozapine-*N*-oxide – saline] for the theta, alpha, beta, and gamma bands).

To measure behavioral arousal, we used the time to return of righting reflex (or time to return of movement if righting reflex was not lost; see "Materials and Methods") as a surrogate for recovery from anesthesia. In contrast to the reduced delta oscillations, the recovery times between clozapine-*N*-oxide and saline conditions did not show statistically significant differences (fig. 3C; median difference [clozapine-*N*-oxide – saline] = 1.63 min, 95% CI = –20.06 to 14.14 min, P = 0.945; N = 8 male rats).

We next sought to understand whether excitation of CaMKIIa$^+$ parabrachial nucleus region neurons also reduces delta power effectively at a higher dose of dexmedetomidine. In these experiments, after injection of clozapine-*N*-oxide, we administered high-dose dexmedetomidine (4.5 $\mu g \cdot kg^{-1} \cdot min^{-1}$ for 10 min). We found that other than one short period with lower delta power from 6 to 8 min, delta power in the prefrontal EEG during the infusion did not show statistically significant differences relative to control experiments in the same rats with saline injections. After the infusion, periods with lower delta power with parabrachial nucleus region stimulation appeared from 60 to 64 min, 78 to 98 min, 108 to 110 min, and 112 to 118 min (fig. 4, A and B; trace in fig. 4B summarizes delta power with clozapine-*N*-oxide injections minus delta power with

saline injections, and periods with CIs that do not span zero show statistically significant differences with 99% confidence; peak statistically significant median bootstrapped difference in power during dexmedetomidine infusion [clozapine-*N*-oxide – saline] = –1.93 dB, 99% CI = –4.16 to –0.56 dB, $P = 0.006$, N = 7 male rats; for the entire trace in fig. 4B, N = 7 male rats). Power in the theta, alpha, and beta bands decreased with clozapine-*N*-oxide injections relative to saline injections, although to a lesser degree than with low-dose dexmedetomidine. Conversely, power in the gamma band increased after the dexmedetomidine infusion was completed (see Supplemental Digital Content 4, http://links.lww.com/ALN/C651, which shows the summary power differences [clozapine-*N*-oxide – saline] for the theta, alpha, beta, and gamma bands).

As with low-dose dexmedetomidine, recovery after high-dose dexmedetomidine infusion, as measured by the return of righting reflex, did not show statistically significant differences for rats with clozapine-*N*-oxide injections relative to saline controls (fig. 4C; median difference [clozapine-*N*-oxide – saline] = 11.01 min, 95% CI = –20.84 to 23.67 min, $P = 0.297$; N = 7 male rats).

Excitation of CaMKIIa$^+$ Neurons in the Parabrachial Nucleus Region Fails to Reduce Delta Power during Ketamine Anesthesia and Increases Time to Recovery from High-dose Ketamine

Given that excitation of CaMKIIa$^+$ parabrachial nucleus region neurons reduced low-dose dexmedetomidine-induced delta power, we next tested whether stimulation of these same neurons could reduce ketamine-induced delta power. In these experiments, 1 h after injection of clozapine-*N*-oxide, we administered ketamine (2 mg · kg^{-1} · min^{-1} for 30 min). At this dose, all rats lost the righting reflex, although many rats moved when they were placed on their sides (6 of 7 male rats moved with control conditions; 2 of 7 male rats moved with clozapine-*N*-oxide conditions). In contrast with low-dose dexmedetomidine, for low-dose ketamine, delta power in the prefrontal EEG during the infusion did not show statistically significant differences relative to control experiments in the same rats with saline injections. After the infusion, periods with lower delta power with clozapine-*N*-oxide injections appeared from 64 to 68 min, 70 to 74 min, 78 to 82 min, 84 to 86 min, 90 to 96 min, 110 to 112 min, and 114 to 116 min. In addition, one brief period with higher delta power appeared from 44 to 46 min (fig. 5, A and B; trace in fig. 5B summarizes delta power with clozapine-*N*-oxide injections minus delta power with saline injections, and periods with CIs that do not span zero show statistically significant differences with 99% confidence; for the entire trace in fig. 5B, N = 6 to 7 male rats). During the ketamine infusion, there was a brief decrease in theta power but no differences in alpha, beta, and gamma power with clozapine-*N*-oxide injections relative to saline injections. After the infusion, theta, alpha, and gamma showed brief periods of decreased power, theta showed a brief increase in power, and beta showed no differences (see Supplemental Digital Content 5, http://links.lww.com/ALN/C652, which shows the summary power differences [clozapine-*N*-oxide – saline] for the theta, alpha, beta, and gamma bands).

Similar to dexmedetomidine, recovery after low-dose ketamine infusion, as measured by the return of righting reflex, did not show statistically significant differences for rats with clozapine-*N*-oxide injections relative to saline controls (fig. 5C; median difference [clozapine-*N*-oxide – saline] = 12.82 min, 95% CI = –3.20 to 39.58 min, $P = 0.109$; N = 7 male rats).

When a higher dose of ketamine (4 mg · kg^{-1} · min^{-1} for 15 min) was used, excitation of CaMKIIa$^+$ parabrachial nucleus region neurons (*via* clozapine-*N*-oxide injections) had little effect on delta power in the prefrontal EEG during the infusion, except for a brief reduction in power from 0 to 2 min. After the infusion, periods with lower delta power with parabrachial nucleus region stimulation appeared from 52 to 54 and 62 to 66 min (fig. 6, A and B; trace in fig. 6B summarizes delta power with clozapine-*N*-oxide injections minus delta power with saline injections, and periods with CIs that do not span zero show statistically significant differences with 99% confidence; peak statistically significant median bootstrapped difference in power during ketamine infusion [clozapine-*N*-oxide – saline] = –0.87 dB, 99% CI = –1.62 to –0.18 dB, $P = 0.019$, N = 8 male rats; for the entire trace in fig. 6B, N = 7 to 8 male rats). During the ketamine infusion, power in the theta, alpha, beta, and gamma bands showed no differences with clozapine-*N*-oxide injections relative to saline injections. After the infusion, theta and beta showed brief periods of decreased power, and alpha and beta showed some increased power. No differences were seen in gamma power (see Supplemental Digital Content 6, http://links.lww.com/ALN/C653, which shows the summary power differences [clozapine-*N*-oxide – saline] for the theta, alpha, beta, and gamma bands).

However, contrary to the rest of the anesthesia conditions, recovery after high-dose ketamine infusion, as measured by the return of righting reflex, was *longer* for rats with clozapine-*N*-oxide injections relative to saline controls. This elongation of recovery times was statistically significant (fig. 6C; median difference [clozapine-*N*-oxide – saline] = 11.38 min, 95% CI = 1.81 to 24.67 min, $P = 0.016$; N = 8 male rats).

Discussion

In this study, the primary outcome was evidence that excitation of putative glutamatergic neurons in the parabrachial nucleus region is sufficient to reduce delta power during low-dose dexmedetomidine anesthesia but not high-dose dexmedetomidine nor ketamine anesthesia. Furthermore, changes in delta power did not correspond to changes in

time to recovery from anesthesia. As a secondary outcome, we found that selectively stimulating putative glutamatergic neurons in the parabrachial nucleus region was sufficient to reduce delta power and time spent in sleep without anesthesia. We also found lesser effects of parabrachial nucleus region stimulation on other frequency bands, including theta, alpha, beta, and gamma, with and without anesthesia. These results advance our understanding of the neural circuit mechanisms underlying EEG patterns under anesthesia and may be useful for improving clinical EEG monitors.

Limitation of Using a Single Biologic Sex

We used male rats in our study so that our results would be comparable to previous studies that used male rodents to examine the effects of parabrachial nucleus stimulation during anesthesia.[2,5,8,10] We cannot rule out, however, that there may be sex differences in the neurophysiologic or behavioral responses to parabrachial nucleus stimulation. Future studies that include both and compare between the sexes are recommended to discern any potential differences.

Limitation of Targeting DREADDs to CaMKIIa$^+$ Neurons

The extent of colocalization of CaMKIIa expression with glutamatergic neurons in the parabrachial nucleus has not been studied, so it is not known whether all DREADDs$^+$ neurons in our study were glutamatergic. However, previous studies have shown a strong association between CaMKIIa$^+$ and glutamatergic neurons in the cortex,[33,34] amygdala,[35] and thalamus,[36] as well as a strong disassociation between CaMKIIa$^+$ and GABAergic neurons in the basal ganglia, thalamus, and hypothalamus.[37] The parabrachial nucleus has also been shown to be primarily glutamatergic[18] and express CaMKII.[38,39] These previous findings, combined with the large extent of CaMKIIa-driven expression of DREADDs in the parabrachial nucleus in our study, are consistent with the claim that the majority of our DREADDs$^+$ neurons were glutamatergic.

Return of Righting Reflex as a Measure of Recovery

In our study, we did not observe any statistically significant reduction in recovery times with clozapine-*N*-oxide injections relative to saline injections. Contrary to our expectations, we found an *increase* in time to recovery with excitation of parabrachial nucleus region neurons in the case of high-dose ketamine. This result could indicate a disconnect between neurophysiologic and behavioral indicators of arousal. Indeed, the righting reflex itself does not involve cortical activity[40] and presumably would not directly affect the EEG. However, there are also other possibilities that should be considered. First, because of the arousable nature of low-dose anesthesia (in particular, dexmedetomidine anesthesia) and the large SD of recovery times even under controlled conditions, the return of righting reflex can be a variable, albeit common measure of behavioral arousal. In addition, during recovery from dexmedetomidine, although a rat may recover from anesthesia enough to return to the upright position, they usually quickly return to an unconscious state, with the recovery time period lasting far beyond the initial arousal. Finally, in the experiments without anesthesia, a subset of rats showed very little movement after clozapine-*N*-oxide injection, despite lack of sleep (see example in fig. 2B). This stillness with DREADDs stimulation did not correspond in any obvious way to differences in the anatomical regions expressing DREADDs. However, if this behavior was present as anesthesia began to wear off, it could have confounded the time-to-recovery results.

Parabrachial Nucleus Region Stimulation Has Minor Effects on Theta, Alpha, Beta, and Gamma Bands

Although not the primary outcome, we also found some differences in the theta, alpha, beta, and gamma bands with parabrachial nucleus region stimulation. In experiments without anesthesia, reduced amounts of sleep with clozapine-*N*-oxide injections may be responsible for broadband power reductions affecting the theta, alpha, and beta bands, in addition to delta. The reduced amount of sleep with clozapine-*N*-oxide injections is also consistent with increased gamma power, because gamma power decreases with sleep.[41]

Power during the dexmedetomidine anesthesia experiments largely follows the same pattern as the sleep experiments. The reductions in theta, alpha, and beta and the increase in gamma suggest a similar effect of parabrachial nucleus region stimulation on dexmedetomidine anesthesia and sleep and may underscore similarities in their mechanisms. For ketamine anesthesia experiments, most changes in power occur after the anesthesia infusion has completed, while the rats are recovering. Thus, the minor changes that we observed may have more to do with the return of sleeping behavior than with an interaction between parabrachial nucleus region stimulation and ketamine.

Differences in Response to Parabrachial Nucleus Region Excitation May Reflect Different Delta Mechanisms

We found that the ability of CaMKIIa$^+$ neuron excitation in the parabrachial nucleus region to promote arousal during concurrent anesthesia depended on the molecular targets of the anesthetics. In particular, excitation of these neurons reduced delta oscillations during dexmedetomidine (fig. 3) but not ketamine anesthesia (figs. 5 and 6). These results may suggest that distinct mechanisms are responsible for delta generation between these two anesthetics.

Anesthetics such as propofol, isoflurane, and sevoflurane enhance or replicate GABAergic neurotransmission in both subcortical and cortical neurons. As a result, the cortex is inhibited both indirectly, because subcortical arousal nuclei provide less excitatory neurotransmission, and directly, because GABAergic neurotransmission onto cortical

neurons is increased.[21,26] Like GABAergic anesthetics, dexmedetomidine exerts both indirect and direct effects on the cortex: (1) Dexmedetomidine inhibits norepinephrine release from the locus coeruleus,[20] which disinhibits the preoptic area (a sleep-active area), leading to indirect inhibition of other major arousal areas and the cortex. (2) Although less studied, α_{2A}-adrenergic receptors also exist in the cortex,[42] and dexmedetomidine may also exert effects on the cortex directly. Similar to the effects of parabrachial nucleus excitation with GABAergic anesthetics, exciting glutamatergic neurons in the parabrachial nucleus may counteract both the indirect and direct cortical inhibition caused by dexmedetomidine, causing neurophysiologic arousal. This would happen as excitatory, glutamatergic projections from the parabrachial nucleus to other subcortical arousal areas and the cortex are activated. When the inhibition is more profound (as with a high dose of dexmedetomidine), the cortical excitation provided by parabrachial nucleus activation is insufficient to overcome the inhibition (fig. 4).

Although ketamine is like GABAergic anesthetics and dexmedetomidine in its inhibition of subcortical arousal areas, it is distinct in its direct cortical effects.[21,26] Ketamine is thought to disinhibit cortical neurons and produce an overall excitatory effect on pyramidal neurons *via* inhibition of local interneurons.[27,28,43] Because excitation of the parabrachial nucleus also has an excitatory effect on the cortex, it likely cannot counteract the direct effects of ketamine on the cortex and thus is ineffective at evoking neurophysiologic arousal. In addition, because ketamine antagonizes NMDA receptors, it may blunt the effects of glutamate release that the parabrachial nucleus provides when excited. It is possible that parabrachial nucleus stimulation may lead to arousal with other doses of ketamine; however, movement was not prevented by the low-dose ketamine we used, so decreasing the dose further would cause insufficient sedation to discern differences between clozapine-*N*-oxide and saline conditions. In addition, because parabrachial nucleus region stimulation did not cause consistent delta power nor recovery time reductions with low-dose or high-dose ketamine, it is unlikely that an even higher dose would be arousable.

Although not examined in this study, it is possible that inhibition of glutamatergic neurons in the parabrachial nucleus increases cortical delta power or the time to recovery from dexmedetomidine or ketamine anesthesia. Indeed, one recent study showed inhibition of glutamatergic parabrachial nucleus neurons increases time to recovery from sevoflurane.[8] However, other studies of parabrachial nucleus excitation have not reported the effects of inhibition on arousal from anesthesia.[2,5] The inability of DREADDs techniques to completely silence (rather than just dampen) neural activity can make interpreting results a challenge.[44] For this reason, we chose not to investigate the effects of inhibition on arousal from anesthesia.

Finally, the balance between inhibition and excitation can be crucial for determining the oscillatory state of neural circuits.[45–48] It is therefore possible that the excitation of glutamatergic neurons in the parabrachial nucleus is effective at disrupting that balance with GABAergic anesthetics and low-dose dexmedetomidine, but it does not disrupt that balance with high-dose dexmedetomidine or ketamine. Consistent with this hypothesis, the parabrachial nucleus projects to the basal forebrain, and accordingly, stimulation of the parabrachial nucleus may cause cortical acetylcholine release. Because dexmedetomidine infusions do not change cortical acetylcholine levels,[49] excitation of the parabrachial nucleus may cause unbalanced cortical excitation *via* an overabundance of acetylcholine, reducing delta power and leading to neurophysiologic arousal. More research, including measurement of cortical neurotransmitters, will be helpful for explaining the mechanisms responsible for the differing responses to excitation of glutamatergic parabrachial nucleus region neurons with these two anesthetics.

Acknowledgments

Statistical support was provided by the Anesthesia Research Center within the Department of Anesthesia, Critical Care and Pain Medicine at Massachusetts General Hospital, Boston, Massachusetts.

Research Support

Supported by grant No. P01-GM118269 from the National Institutes of Health, Bethesda, Maryland, and the Department of Anesthesia, Critical Care and Pain Medicine, Massachusetts General Hospital, Boston, Massachusetts.

Competing Interests

Dr. Solt is a consultant to Takeda Pharmaceuticals (Tokyo, Japan). The other authors declare no competing interests.

Correspondence

Address correspondence to Dr. Melonakos: Massachusetts General Hospital, 149 13th Street, Charlestown, Massachusetts 02129. emelonakos@mgh.harvard.edu.

References

1. Hemmings HC Jr, Riegelhaupt PM, Kelz MB, Solt K, Eckenhoff RG, Orser BA, Goldstein PA: Towards a comprehensive understanding of anesthetic mechanisms of action: A decade of discovery. Trends Pharmacol Sci 2019; 40:464–81
2. Qiu MH, Chen MC, Fuller PM, Lu J: Stimulation of the pontine parabrachial nucleus promotes wakefulness via extra-thalamic forebrain circuit nodes. Curr Biol 2016; 26:2301–12
3. Eban-Rothschild A, Rothschild G, Giardino WJ, Jones JR, de Lecea L: VTA dopaminergic neurons

regulate ethologically relevant sleep-wake behaviors. Nat Neurosci 2016; 19:1356–66
4. Datta S, Siwek DF: Excitation of the brain stem pedunculopontine tegmentum cholinergic cells induces wakefulness and REM sleep. J Neurophysiol 1997; 77:2975–88
5. Luo T, Yu S, Cai S, Zhang Y, Jiao Y, Yu T, Yu W: Parabrachial neurons promote behavior and electroencephalographic arousal from general anesthesia. Front Mol Neurosci 2018; 11:420
6. Solt K, Van Dort CJ, Chemali JJ, Taylor NE, Kenny JD, Brown EN: Electrical stimulation of the ventral tegmental area induces reanimation from general anesthesia. Anesthesiology 2014; 121:311–9
7. Vazey EM, Aston-Jones G: Designer receptor manipulations reveal a role of the locus coeruleus noradrenergic system in isoflurane general anesthesia. Proc Natl Acad Sci U S A 2014; 111:3859–64
8. Wang TX, Xiong B, Xu W, Wei HH, Qu WM, Hong ZY, Huang ZL: Activation of parabrachial nucleus glutamatergic neurons accelerates reanimation from sevoflurane anesthesia in mice. Anesthesiology 2019; 130:106–18
9. Alkire MT, McReynolds JR, Hahn EL, Trivedi AN: Thalamic microinjection of nicotine reverses sevoflurane-induced loss of righting reflex in the rat. Anesthesiology 2007; 107:264–72
10. Muindi F, Kenny JD, Taylor NE, Solt K, Wilson MA, Brown EN, Van Dort CJ: Electrical stimulation of the parabrachial nucleus induces reanimation from isoflurane general anesthesia. Behav Brain Res 2016; 306:20–5
11. Taylor NE, Van Dort CJ, Kenny JD, Pei J, Guidera JA, Vlasov KY, Lee JT, Boyden ES, Brown EN, Solt K: Optogenetic activation of dopamine neurons in the ventral tegmental area induces reanimation from general anesthesia. Proc Natl Acad Sci U S A 2016; 113:12826–31
12. Pal D, Dean JG, Liu T, Li D, Watson CJ, Hudetz AG, Mashour GA: Differential role of prefrontal and parietal cortices in controlling level of consciousness. Curr Biol 2018; 28:2145–52.e5
13. Solt K, Cotten JF, Cimenser A, Wong KF, Chemali JJ, Brown EN: Methylphenidate actively induces emergence from general anesthesia. Anesthesiology 2011; 115:791–803
14. Chemali JJ, Van Dort CJ, Brown EN, Solt K: Active emergence from propofol general anesthesia is induced by methylphenidate. Anesthesiology 2012; 116:998–1005
15. Kenny JD, Chemali JJ, Cotten JF, Van Dort CJ, Kim SE, Ba D, Taylor NE, Brown EN, Solt K: Physostigmine and methylphenidate induce distinct arousal states during isoflurane general anesthesia in rats. Anesth Analg 2016; 123:1210–9
16. Kenny JD, Taylor NE, Brown EN, Solt K: Dextroamphetamine (but not atomoxetine) induces reanimation from general anesthesia: Implications for the roles of dopamine and norepinephrine in active emergence. PLoS One 2015; 10:e0131914
17. Kelz MB, García PS, Mashour GA, Solt K: Escape from oblivion: Neural mechanisms of emergence from general anesthesia. Anesth Analg 2019; 128:726–36
18. Fuller PM, Fuller P, Sherman D, Pedersen NP, Saper CB, Lu J: Reassessment of the structural basis of the ascending arousal system. J Comp Neurol 2011; 519:933–56
19. Fulwiler CE, Saper CB: Subnuclear organization of the efferent connections of the parabrachial nucleus in the rat. Brain Res 1984; 319:229–59
20. Nelson LE, Lu J, Guo T, Saper CB, Franks NP, Maze M: The α2-adrenoceptor agonist dexmedetomidine converges on an endogenous sleep-promoting pathway to exert its sedative effects. Anesthesiology 2003; 98:428–36
21. Brown EN, Purdon PL, Van Dort CJ: General anesthesia and altered states of arousal: A systems neuroscience analysis. Annu Rev Neurosci 2011; 34:601–28
22. McCarren HS, Chalifoux MR, Han B, Moore JT, Meng QC, Baron-Hionis N, Sedigh-Sarvestani M, Contreras D, Beck SG, Kelz MB: α2-Adrenergic stimulation of the ventrolateral preoptic nucleus destabilizes the anesthetic state. J Neurosci 2014; 34:16385–96
23. Zhang Z, Ferretti V, Güntan İ, Moro A, Steinberg EA, Ye Z, Zecharia AY, Yu X, Vyssotski AL, Brickley SG, Yustos R, Pillidge ZE, Harding EC, Wisden W, Franks NP: Neuronal ensembles sufficient for recovery sleep and the sedative actions of α2 adrenergic agonists. Nat Neurosci 2015; 18:553–61
24. Hu FY, Hanna GM, Han W, Mardini F, Thomas SA, Wyner AJ, Kelz MB: Hypnotic hypersensitivity to volatile anesthetics and dexmedetomidine in dopamine β-hydroxylase knockout mice. Anesthesiology 2012; 117:1006–17
25. Boon JA, Milsom WK: NMDA receptor-mediated processes in the Parabrachial/Kölliker fuse complex influence respiratory responses directly and indirectly via changes in cortical activation state. Respir Physiol Neurobiol 2008; 162:63–72
26. Brown EN, Pavone KJ, Naranjo M: Multimodal general anesthesia: Theory and practice. Anesth Analg 2018; 127:1246–58
27. Homayoun H, Moghaddam B: NMDA receptor hypofunction produces opposite effects on prefrontal cortex interneurons and pyramidal neurons. J Neurosci 2007; 27:11496–500
28. Ali F, Gerhard DM, Sweasy K, Pothula S, Pittenger C, Duman RS, Kwan AC: Ketamine disinhibits dendrites and enhances calcium signals in prefrontal dendritic spines. Nat Commun 2020; 11:72
29. Melonakos ED, Moody OA, Nikolaeva K, Kato R, Nehs CJ, Solt K: Manipulating neural circuits in anesthesia research. Anesthesiology 2020; 133:19–30

30. Alexander GM, Rogan SC, Abbas AI, Armbruster BN, Pei Y, Allen JA, Nonneman RJ, Hartmann J, Moy SS, Nicolelis MA, McNamara JO, Roth BL: Remote control of neuronal activity in transgenic mice expressing evolved G protein–coupled receptors. Neuron 2009; 63:27–39
31. Prerau MJ, Brown RE, Bianchi MT, Ellenbogen JM, Purdon PL: Sleep Neurophysiological dynamics through the lens of multitaper spectral analysis. Physiology (Bethesda) 2017; 32:60–92
32. Schindelin J, Arganda-Carreras I, Frise E, Kaynig V, Longair M, Pietzsch T, Preibisch S, Rueden C, Saalfeld S, Schmid B, Tinevez JY, White DJ, Hartenstein V, Eliceiri K, Tomancak P, Cardona A: Fiji: An open-source platform for biological-image analysis. Nat Methods 2012; 9:676–82
33. Jones EG, Huntley GW, Benson DL: α-Calcium/calmodulin-dependent protein kinase II selectively expressed in a subpopulation of excitatory neurons in monkey sensory-motor cortex: Comparison with GAD-67 expression. J Neurosci 1994; 14:611–29
34. Zou DJ, Greer CA, Firestein S: Expression pattern of α CaMKII in the mouse main olfactory bulb. J Comp Neurol 2002; 443:226–36
35. McDonald AJ, Muller JF, Mascagni F: GABAergic innervation of α type II calcium/calmodulin-dependent protein kinase immunoreactive pyramidal neurons in the rat basolateral amygdala. J Comp Neurol 2002; 446:199–218
36. Liu XB, Jones EG: Localization of α type II calcium calmodulin-dependent protein kinase at glutamatergic but not γ-aminobutyric acid (GABAergic) synapses in thalamus and cerebral cortex. Proc Natl Acad Sci U S A 1996; 93:7332–6
37. Benson DL, Isackson PJ, Hendry SH, Jones EG: Differential gene expression for glutamic acid decarboxylase and type II calcium-calmodulin-dependent protein kinase in basal ganglia, thalamus, and hypothalamus of the monkey. J Neurosci 1991; 11:1540–64
38. Wang X, Zhang C, Szábo G, Sun QQ: Distribution of CaMKIIα expression in the brain *in vivo*, studied by CaMKIIα-GFP mice. Brain Res 2013; 1518:9–25
39. Hermanson O, Larhammar D, Blomqvist A: Preprocholecystokinin mRNA-expressing neurons in the rat parabrachial nucleus: Subnuclear localization, efferent projection, and expression of nociceptive-related intracellular signaling substances. J Comp Neurol 1998; 400:255–70
40. Wenzel DG, Lal H: The relative reliability of the escape reaction and righting-reflex sleeping times in the mouse. J Am Pharm Assoc Am Pharm Assoc 1959; 48:90–1
41. Adamantidis AR, Gutierrez Herrera C, Gent TC: Oscillating circuitries in the sleeping brain. Nat Rev Neurosci 2019; 20:746–62
42. Scheinin M, Lomasney JW, Hayden-Hixson DM, Schambra UB, Caron MG, Lefkowitz RJ, Fremeau RT: Distribution of α2-adrenergic receptor subtype gene expression in rat brain. Mol Brain Res 1994; 21:133–49
43. Seamans J: Losing inhibition with ketamine. Nat Chem Biol 2008; 4:91–3
44. Smith KS, Bucci DJ, Luikart BW, Mahler SV: DREADDs: Use and application in behavioral neuroscience. Behav Neurosci 2016; 130:137–55
45. Melonakos ED, White JA, Fernandez FR: A model of cholinergic suppression of hippocampal ripples through disruption of balanced excitation/inhibition. Hippocampus 2019; 29:773–86
46. Niethard N, Hasegawa M, Itokazu T, Oyanedel CN, Born J, Sato TR: Sleep-stage–specific regulation of cortical excitation and inhibition. Curr Biol 2016; 26:2739–49
47. Haider B, Duque A, Hasenstaub AR, McCormick DA: Neocortical network activity *in vivo* is generated through a dynamic balance of excitation and inhibition. J Neurosci 2006; 26:4535–45
48. Dehghani N, Peyrache A, Telenczuk B, Le Van Quyen M, Halgren E, Cash SS, Hatsopoulos NG, Destexhe A: Dynamic balance of excitation and inhibition in human and monkey neocortex. Sci Rep 2016; 6:23176
49. Nemoto C, Murakawa M, Hakozaki T, Imaizumi T, Isosu T, Obara S: Effects of dexmedetomidine, midazolam, and propofol on acetylcholine release in the rat cerebral cortex *in vivo*. J Anesth 2013; 27:771–4